Experimental and numerical analysis of the drainage of aluminium foams

2005 J. Phys.: Condens. Matter 17 6353

(http://iopscience.iop.org/0953-8984/17/41/006)

INSTITUTE OF PHYSICS PUBLISHING JOURNAL OF PHYSICS: CONDENSED MATTER

J. Phys.: Condens. Matter **17** (2005) 6353–6362 doi:10.1088/0953-8984/17/41/006

Experimental and numerical analysis of the drainage of aluminium foams

O Brunke[1], A Hamann[1], S J Cox[2,3] and S Odenbach[1]

[1] ZARM Universität Bremen, Am Fallturm, 28359 Bremen, Germany
[2] Department of Physics, Trinity College, Dublin 2, Republic of Ireland

Received 23 February 2005, in final form 28 June 2005
Published 30 September 2005
Online at stacks.iop.org/JPhysCM/17/6353

Abstract

Drainage is one of the driving forces for the temporal instability of molten metal foams. For usual aqueous foams this phenomenon is well examined and understood on both the experimental and the theoretical side. The situation is different for metallic foams. Due to their opaque nature, the observation of drainage is only possible by either measuring the density distribution of solidified samples *ex situ* or by x-ray or neutron radioscopy. Up to now there exists just one theoretical study describing the drainage behaviour of metallic foams incorporating the drainage equation, the temperature dependence of the viscosity and thermal transport. This paper will present results on the drainage behaviour of aluminium foams grown by a powder-metallurgical production route. For this purpose an experiment which allows the observation of drainage in cylindrical metal foam columns has been developed. Experimental density profiles after different drainage times are measured *ex situ* and compared to numerical results of the standard drainage equation for aqueous foams. This first comparison between the density redistribution of metallic aluminium foams and numerical solutions shows that the standard drainage equation can be used to explain the drainage behaviour of metallic foams.

(Some figures in this article are in colour only in the electronic version)

1. Introduction

Metallic foams, especially those made from aluminium and its alloys, have become a major topic for both industrial and basic research throughout the last decade. Their unique combination of highly interesting physical properties, like a favourable stiffness to weight ratio, excellent energy absorption capabilities and low flammability, make them an extremely appropriate material for many industrial applications, mainly in the automotive and aerospace

[3] Present address: Institute of Mathematical and Physical Sciences, University of Wales Aberystwyth, Ceredigion SY23 3BZ, UK.

industries [1, 2]. The physical properties of the solid foam which are relevant for most applications are strongly affected by its structure parameters, for instance pore size, shape and distribution, the location of inhomogeneities or the distribution of solid material between films and plateau borders. On the other hand, these parameters directly depend on the temporal development, stability and ageing of the liquid foam system. The major driving phenomenon for the structural changes of foams is gravity-driven drainage and the associated redistribution of metal melt inside the samples.

The drainage behaviour of metallic foams has been observed qualitatively by means of neutron and x-ray radioscopy [3, 4]. Two numerical studies regarding this subject have been published; the first describes the drainage behaviour incorporating the foam drainage equation (FDE) (see e.g. [5, 6]), the temperature dependence of the viscosity and thermal transport [7]. The FDE has successfully described the drainage of aqueous foams [8, 9] but it has not been directly compared with the drainage process in metallic foams.

Secondly, recent work by Gergely and Clyne [10] described a numerical model including liquid not only in the network of the plateau borders (PBs) but also inside the films. It also gives a first comparison of numerics with some experimental drainage data for metallic foams, showing reasonable agreement despite its neglect of a temperature dependent viscosity and thermal transport.

Nonetheless, the experimental testing of the standard FDE for the case of metallic foams has not been performed so far. Therefore, this study has two major goals: a reliable experimental observation of the drainage behaviour as well as a comparison with the one-dimensional prediction of the drainage equation for the case of metallic foams. In the present paper an experiment for the analysis of the drainage of metallic foams produced by a powder metallurgical route is introduced. Combined analyses of cross-sectional images as well as tomographic datasets of the foam samples provide information about the geometric properties of the foam structure. This information is used to give input parameters for the numerical solution of the FDE.

As will be shown in section 4, a first comparison between the observed numerical and experimental drainage data gives reasonable agreement.

2. The foam drainage equation

Free drainage is the redistribution of liquid within an initially homogeneous column of foam due to both a vertical gravitational field and surface-tension-driven capillary effects. A complete description of the foam drainage equation can be found elsewhere [5]; only the key features will be briefly reviewed here and the most important parameters described. The main assumption for the derivation of the drainage equation is the neglect of the contribution of films or cell faces to drainage. It also assumes that the foam is relatively dry, so that the effects of the junctions where the PBs meet can be neglected. This means there is just a flow of liquid through long narrow PBs.

The density ρ_{foam} of a foam and thus its liquid content can be connected to the cross-sectional area A_{PB} of the PBs and the mean cell volume V_{cell} as follows:

$$\rho_{\mathrm{foam}}(z,t) = \rho_{\mathrm{Al}}\phi_{\mathrm{l}} = \rho_{\mathrm{Al}}\left[5.35\frac{A_{\mathrm{PB}}}{V_{\mathrm{Cell}}^{2/3}}\right]. \tag{1}$$

The assumption that no liquid is present in the films works well for aqueous foams [8] but has to be reconsidered when using the FDE for metallic foams, as will be discussed in section 4.3. Combining the continuity equation for incompressible fluids and no-slip boundary conditions

on the PB walls, i.e. Poiseuille flow, gives

$$\frac{\partial A_{\mathrm{PB}}}{\partial t} + \frac{1}{3 f \eta} \frac{\partial}{\partial z} \left(\rho g A_{\mathrm{PB}}^2 - \frac{C\gamma}{2} \sqrt{A_{\mathrm{PB}}} \frac{\partial A_{\mathrm{PB}}}{\partial z} \right) = 0. \tag{2}$$

Equation (2) is known as the foam drainage equation; it is a nonlinear partial differential equation for the liquid content ϕ_{l} or the PB area A_{PB}. In the case of a constant inflow of liquid from the top of the foam column and constant outflow at the bottom, solving (2) gives the expected trivial solution of a constant liquid content. For the free drainage case, i.e. no liquid entering the foam column at the top and leaving it at the bottom, the equation has to be solved numerically to obtain a full solution. For the present work the equation has been solved using explicit finite differences with a constant step size in both space and time, as done in [7] for example. In order to be able to compare the numerical solution with the experimental results, the input parameters f, C, V_{cell} and/or A_{PB}, γ, ρ and η have to be known. The quantities f and C are well known parameters [5], with $f \approx 49$ describing the viscous drag in a channel having the concave triangular shape of an ideal PB cross-section. As will be seen in section 4.1, the typical PB cross-section in a real metallic foam generally has a comparable shape. Thus taking the standard value of $f = 49$ is a reasonable approximation.

Finally, the parameter C is defined as the relation between the radius r_{PB} and area of a PB, $C^2 = A_{\mathrm{PB}}/r_{\mathrm{PB}}^2$. From geometrical considerations it follows that $C^2 = \sqrt{3} - \pi/2 \approx 0.161$.

The values for the thermo-physical properties viscosity η and surface tension γ of liquid metals have either to be measured or taken from the literature. The most critical geometric parameters are the area of PBs and the mean cell volume; the direct measurement of these quantities is not possible for the case of liquid metallic foams. Nonetheless, approximate values can be obtained from solidified samples by means of e.g. analysis of cross-sectional images or tomographic examination [11, 12].

3. Experimental procedures

3.1. Precursor preparation

The foam samples for the present study have been produced by means of a powder metallurgical process, developed by the Fraunhofer institute IFAM in Bremen [1]. The route comprises two steps. The first is the preparation of the precursor material by mixing metal and blowing agent powder and the second is the production of the actual foam. The precursor material has been produced at Schunk Sintermetalltechnik GmbH (Gießen, Germany). An aluminium powder (grain radius $r < 160\ \mu$m) was mixed with silicon powder ($r < 160\ \mu$m) in a weight ratio of 93:7, resulting in an alloy comparable to commercial A356 (AlSi7). Afterwards, 0.6 wt% of TiH_2 was added to serve as the blowing agent. To finally obtain the dense precursor material, this mixture was compacted by extrusion moulding at about 350 °C. The final step to produce the foam is the melting of the precursor in a furnace. The blowing agent releases its hydrogen and generates a foam-like melt. In order to conserve this porous structure the samples are cooled down below their melting point.

3.2. Foaming and drainage set-up

Though the production of metallic foams by means of the powder metallurgical (PM) route is generally simple compared to direct production routes from the melt like CYMAT [2], there is one severe problem in this context, namely the coincidence of expansion and drainage during the initial phase of the foam sample generation. Due to the low porosity i.e. high liquid content at the beginning of the foaming, drainage must mostly occur in this phase. Thus, in order to

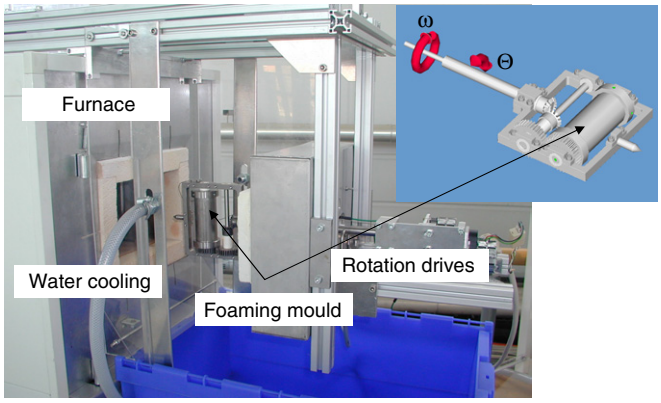

Figure 1. Image of the furnace system for the observation of the drainage behaviour of metallic foams. The inset shows the cylindrical stainless steel foaming mould mounted on the two-axis (ω, θ) sample manipulator.

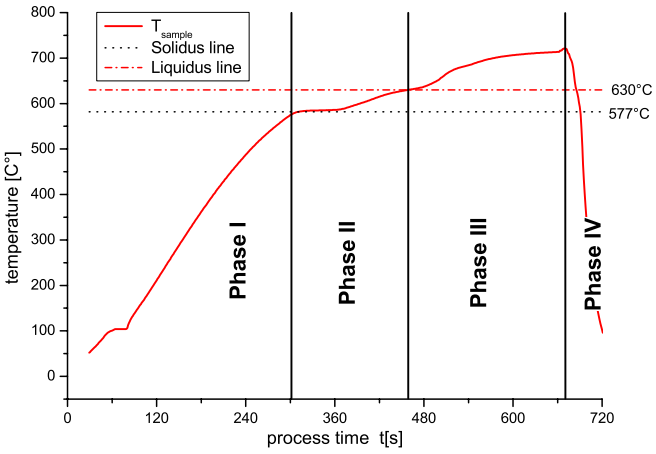

Figure 2. Plot of a typical run of the sample temperature for a complete foaming and drainage experiment. The process is divided into four main phases which are used to control the sample position. Details are given in the text.

generate a simplified experimental situation comparable to the case of the drainage equation (see [7]), the set-up had to be designed to fulfil two main requirements: firstly, the relative density distribution of the initial metallic foam column had to be as homogenous as possible. Secondly, the drainage observation had to be performed on a completely expanded, preferably highly porous (i.e. low liquid content) sample.

Figure 1 shows the furnace system used for the drainage experiments. The precursor samples (diameter 15 mm, length 80 mm) are positioned at the centre of a cylindrical stainless steel mould having a diameter of $d = 30$ mm and a length of $z = 100$ mm. As indicated in the inset too, the container features a two-axis manipulator which allows axial (ω) as well as radial rotation (θ) of the cylindrical foam samples. In order to melt and foam the precursor samples, the whole system is automatically transferred into a standard muffle-type furnace, which provides temperatures up to 1100 °C at spatial homogeneity of ± 1 °C at the sample position. Sample and furnace temperatures are observed by means of K-type thermocouples. The direct monitoring of the sample temperature allows a reliable observation of the sample state and is used to trigger the motor controller of the sample manipulator.

A typical temperature run of a foaming and drainage process is shown in figure 2. The furnace temperature is set to 700 °C and the precursor sample is positioned horizontally $(\theta = 0°)$ inside the furnace chamber (Phase I). Once the solidus temperature for the alloy AlSi7 (577 °C) is reached and the precursor expansion starts, a slow $(\omega = 0.1$ Hz) axial

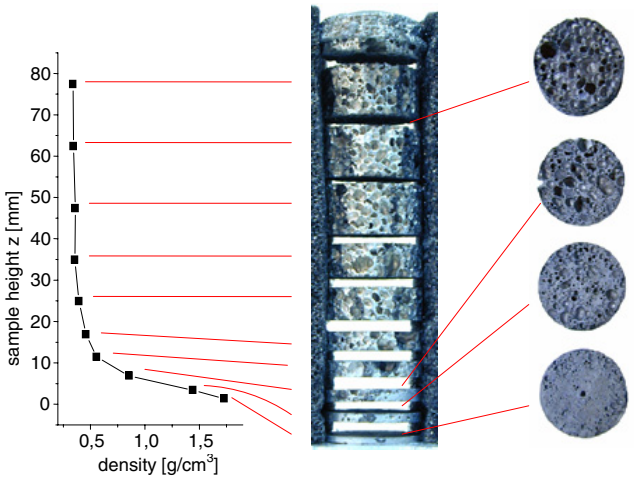

Figure 3. The density profiles of the metallic foam sample are obtained by weighing segments from different heights.

rotation is initiated in order to reduce radial inhomogeneities in density due to drainage effects (Phase II). Ten seconds after reaching the liquidus temperature (630 °C) the foam has reached its maximum volume expansion of about 500%. Now the sample container is placed in a vertical position, and the foam starts to drain along the z-axis of the cylinder (Phase III). Finally, after a given time (e.g. 180 s), the sample is automatically brought out of the furnace and rapidly quenched (within 10 s) to room temperature by means of water cooling (Phase IV). This experimental method allows a reliable and reproducible control of all important experimental parameters. The duration of phase III defines the drainage time and thus allows us to generate density profiles at different steps of the temporal development of the foam structure.

3.3. Sample analysis

The analysis method used to measure the density profiles is straightforward. In order to eliminate effects of the boundary layer between the foam and mould walls, the sample diameter is first reduced by 5 mm by means of turning. Using an electric discharge machine the foam column is separated into cylindrical segments. Their exponentially increasing height from the bottom to the top of the sample is chosen due to the expected density profile. Finally, the density of the segments is determined by weighing. The cut sample and a typical resulting density profile are shown in figure 3.

4. Results and discussion

In order to perform a reasonable comparison between experimental and numerical drainage results, the thermophysical properties, surface tension and viscosity of the liquid alloy have to be known. Furthermore, the geometric parameters of the foam, namely the number of PBs per unit volume, as well as the average cross-sectional area of the PBs have to be determined for the numerical calculations.

4.1. Geometric parameters

The determination was done by 2D image analysis of the cross-sections as well as by the analysis of 3D datasets obtained by means of x-ray microtomography. The experimental set-ups and methods used to determine the mean PB radius r_{PB} and the mean cell volume $\bar{V}_{\mathrm{cell}}$ are

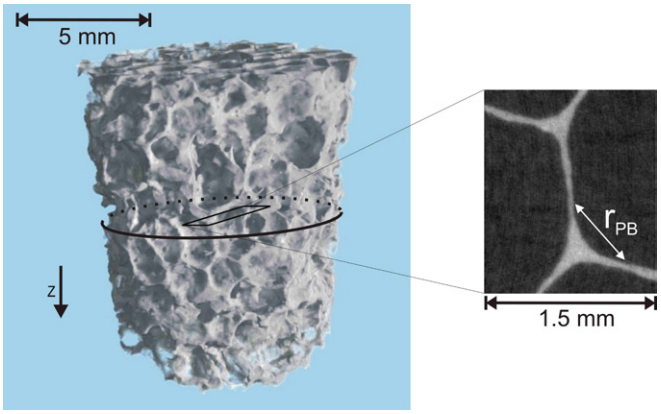

Figure 4. Section of a tomographic dataset of an AlSi7 foam sample produced using the set-up introduced above. The image shows the structure of a foam that was solidified directly after its complete expansion (beginning of phase III) and a part of a slice perpendicular to the z axis. 10 complete slices, as indicated by the circle, at different heights z have been used to determine the initial cross-sectional area of the PBs for the numerical simulations. The mean cell volume has been determined using 3D data analysis methods.

described in [11, 12]. From geometrical considerations presented in [5], the area of a PB can be derived from this value as $A_{\mathrm{PB}} \approx C^2 r_{\mathrm{PB}}^2$ with $C^2 = 0.16$.

Figure 4 shows a cut-out of a tomographic dataset for a foam that was rapidly solidified, immediately after completing phase II. A typical PB and its corresponding approximate radius is also presented. The average cell volume can be determined using methods shown in [11]. The 3D image analysis of the dataset shown in figure 4 yields a mean cell volume of $\bar{V}_{\mathrm{cell}} = 0.47\ \mathrm{mm}^3$. The mean PB radius of this sample is $r_{\mathrm{PB}} = 0.35 \pm 0.15$ mm, giving a mean PB area of $A_{\mathrm{PB}} = (2.0 \pm 0.8) \times 10^{-4}\ \mathrm{cm}^2$. Additionally, the PB radius can be calculated using equation (1), if the relative foam density, and thus the liquid content, is known. For the sample in figure 4, the liquid content is $\phi_{\mathrm{l}} \approx 0.20$, so using equation (1) results in $r_{\mathrm{PB}} \approx 0.37$ mm, which shows a very good agreement with the value obtained by analysing slices of the tomographic foam dataset.

4.2. Thermophysical parameters

The viscosity of liquid metals can be measured by means of an oscillating vessel viscometer. This method measures the damping of the oscillation of a cylindrical container filled with liquid. The damping caused by the viscous friction can be used to determine the viscosity of the liquid inside the container. The viscosity of metals depends critically on the composition of the alloy, the content of solid particles like e.g. AlO_x and the temperature of the liquid. Therefore the temperature-dependent viscosity for the precursor alloy AlSi7 with an oxide content of about 0.5% has been measured and compared to the values for pure (>99.995) cast Al and AlSi7 samples. At the default foaming temperature (700 °C) the resulting values for the viscosities are $\eta_{\mathrm{precur}}(700\,^{\circ}\mathrm{C}) = 1.7 \pm 0.1$ mPa s for the AlSi7 foam precursor material, $\eta_{\mathrm{AlSi7}}(700\,^{\circ}\mathrm{C}) = 1.2 \pm 0.1$ mPa s for pure AlSi7, and $\eta_{\mathrm{Al}}(700\,^{\circ}\mathrm{C}) = 1.4 \pm 0.1$ mPa s for pure aluminium. The value for pure aluminium shows excellent agreement with the measured results of other publications [13]. The measured results clearly indicate a strong dependence of the bulk viscosity of AlSi7 on the oxide content; it increases by a factor of ≈1.4. The value for the surface tension has been taken from the literature. At 700 °C the surface tension of AlSi7 alloys is reported to be $\sigma_{\mathrm{AlSi7}} = 0.8\ \mathrm{N\ m}^{-1}$ [14].

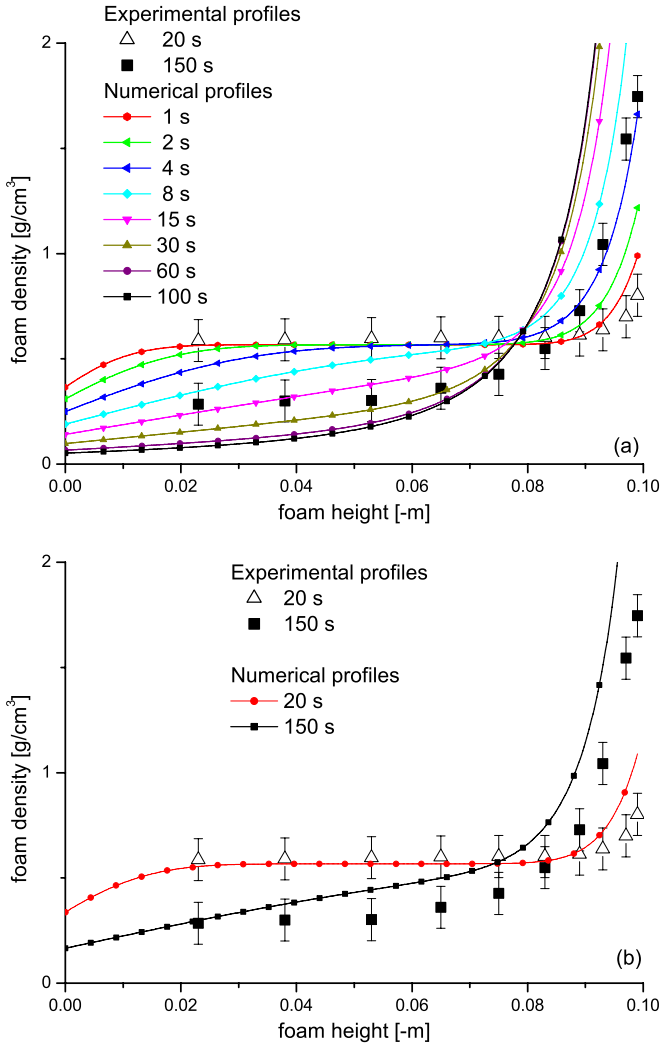

Figure 5. Solutions of the FDE using an initial, uniform, liquid content of $\phi_l \approx 0.20$ as calculated from the measured values for PB area and mean cell volume. (a) Values for the thermophysical parameters are taken as given in section 4.2. (b) The viscosity has been increased by a factor of 10 in order to match the experimental results.

4.3. Numerical and experimental drainage results

The result of the experimental foam density profiles after different drainage times is shown in figure 5. The error bars given for the experimental data represent the standard deviation of four measured drainage profiles. The small error bars indicate the good reproducibility of the experimental procedure. Looking at the data of the samples with a drainage time of 20 s, the capability of the set-up to generate an initially homogeneous density profile can be seen.

In order to show whether the standard FDE can be used to explain the drainage behaviour of liquid metallic foams with a relatively high liquid content, different approaches have been used which will be described in the following section. For all cases the FDE has been solved numerically with no inflow/outflow boundary conditions at the top and bottom of the foam column.

The numerical results in figure 5(a) have been obtained as follows: firstly the values for the thermophysical properties of the AlSi7 precursor have to be provided as input parameters. As stated above, the viscosity of the precursor has been measured and the surface tension is known from literature. Secondly, the structure parameters of the foam have to be determined as described in section 4.1. The resulting value for the area of the PBs is $A_{\mathrm{PB}} = (2.0 \pm 1.5) \times 10^{-4}$ cm^2. As stated in section 4.1 the mean cell volume obtained from the analysis of the tomographic dataset is $V_{\mathrm{cell}} = 0.47 \pm 0.3$ mm^3, so, using equation (1), the resulting liquid content is $\phi_{\mathrm{l}} = 0.22 \pm 0.1$. Taking the measured initial density of the foam as $\rho_{\mathrm{foam}} = 0.55$ g cm^{-3}, the initial liquid content can be determined directly to be $\phi_{\mathrm{l}} \approx 0.20$, which shows very good agreement with the value obtained using equation (1).

Due to the low viscosity and the large PB area the drainage is very fast and already reaches the equilibrium profile after about 100 s, which is about an order of magnitude faster than in the experiments. The increase of the bulk viscosity of the foam material by a factor of ≈1.4 due to the oxide content is thus not sufficient to explain the slow drainage behaviour and relatively long stability of the foam. To account for the much slower process, a higher effective viscosity $\eta^* \sim \eta_{\mathrm{AlSi}} \times 10$ has been taken in order to reduce the simulated drainage rate. The resulting profiles are given in figure 5(b). The necessity to increase the viscosity by about one order of magnitude could be explained by two facts. (i) On the one hand the viscosity has been determined for the bulk liquid alloy by means of the oscillation vessel method, i.e. no shear rate is applied to the liquid. The rheological behaviour of this complex system consisting of the liquid aluminium alloy and suspended solid oxide particles in thin films has not been analysed and could behave completely differently. (ii) Furthermore, a recent study [15] suggests the formation of a network of oxide particles in metallic foams which could strongly influence the effective viscosity of the system for drainage processes. Such a network could give rise to a non-Newtonian behaviour of the liquid. Comprehensive rheological examinations using e.g. a high-temperature shear-controlled plate–plate rheometer could give a deeper insight into the complex nature of the viscosity of the system.

Not only the viscosity but also the surface tension could strongly deviate from the taken literature values due to the oxide content and other impurities contained in the foam precursor material. Due to the fact that ρg is about five orders of magnitude greater than $C\gamma$ (cf equation (2)) even a variation of the surface tension of more than two orders of magnitude would have a negligible effect on the drainage rate. This means that the timescale of the redistribution of the liquid is not affected, even if there is a strong deviation between the actual and the literature value of the surface tension. On the other hand, the drainage profile, i.e. the shape of the density distribution between the top and the bottom of the foam column, is influenced by surface tension effects. In order to illustrate this behaviour, the surface tension for the drainage simulation has been varied from the literature value. The resulting curves are shown in figure 6. In addition to the numerical profile which corresponds to the literature value of $\sigma_{\mathrm{AlSi7}} = 0.8$ N m^{-1} and the experimental data for a drainage time of 150 s, a reduced ($\sigma = 0.4$ N m^{-1}) as well as an increased ($\sigma = 1.6$ N m^{-1}) surface tension have been assumed to calculate the density distribution. Again, an effective viscosity of $\eta^* \sim \eta_{\mathrm{AlSi}} \times 10$ has been used to obtain the experimental drainage rate.

Varying the surface tension clearly shows that there is a dependence of the shape of the density profiles on the surface tension, especially at the lower part of the foam column. Therefore, the behaviour of both thermophysical parameters—viscosity and surface tension—have to be studied in detail to further improve the understanding of the drainage of metallic foams.

However, using the adopted value for the viscosity the plot shows a reasonable agreement between the numerical and experimental data. This agreement can be taken as a strong hint that

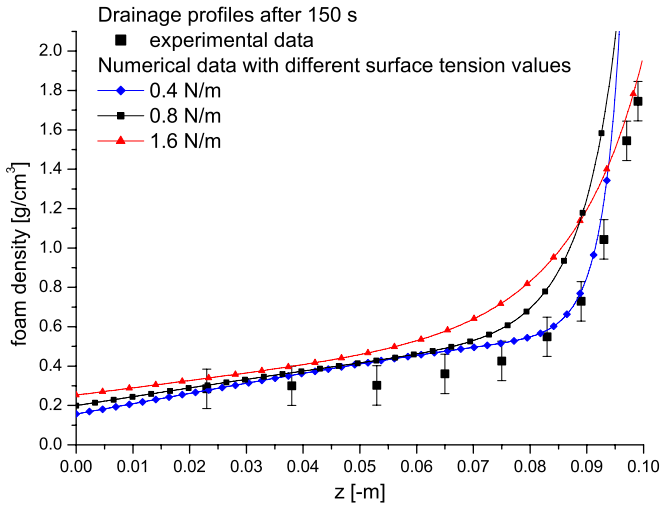

Figure 6. Variation of the numerical density distribution after 150 s drainage time for three different surface tension values showing the influence of this parameter on the shape of the profile.

the above described assumption of a much higher effective viscosity can be used to describe free drainage in metallic foams using the FDE, but the reason for this increase has to be clarified. Additionally, it has to be pointed out that the assumption that the bubble size is constant in space and time is also a simplification, since the structure of a real metallic foam is not static. Furthermore, the FDE does not take into account the effect of the relatively high film thickness (compared to aqueous foams) of at least 30 μm in real Al foams. Regarding this rather simple assumption, the agreement between the numerical and experimental results within the order of magnitude is satisfactory. The standard drainage equation can thus be used as a starting point to understand the general drainage behaviour of metallic foams.

5. Conclusions and outlook

The drainage behaviour of metallic Al foams produced by a powder metallurgical route was observed and compared to numerical results of a variant of the foam drainage equation. In order to be able to obtain reliable data for drainage behaviour of metallic foams, a special set-up was designed, allowing us to observe the drainage at completely expanded and initially homogeneous metallic foams.

As input parameters for the numerical simulation, the mean cell volume and the cross-sectional area of the PBs have been measured by analysing tomography datasets. The viscosity of the liquid precursor material AlSi7 for the foams has been measured by means of the oscillating vessel technique. The value for the surface tension of this material has been taken from the literature.

A good agreement between experimental and numerical drainage profiles could be obtained by using the assumption that the correct drainage rate in the numerical solution is reached by taking an effective viscosity η^* which is about one order of magnitude larger than the measured bulk viscosity of the foam precursor material.

The first comparison between experimental results and numerical calculation shows that the standard FDE can principally be used to describe drainage in metallic foams. But it also becomes obvious that the difference in viscous behaviour, surface tension and density between

liquid metals and water requires an appropriate adjustment of the parameters used for the calculations.

In the near future the experimental procedure will be extended to observe the drainage behaviour of metallic foams *in situ* by means of an x-ray radioscopy set-up. The sample holder is equipped with a two-axis sample manipulator comparable to the one presented in this study, allowing the experimental procedure to be performed under the same reliable conditions but with the addition of a direct time-dependent drainage analysis. On the numerical side, a variable bubble size will be included into the drainage equation in the future. The contribution of film drainage to the drainage rate, due to the non-infinitesimal film thickness, could also be taken into account [16, 17]. Finally, the model of Gergely and Clyne [10] could be compared to the experimental observations. The model of Neethling [18], in which drag parameters for each part of the foam's structure are fitted to the experimental result, may shed light on the importance of the drainage in the PB junctions.

Acknowledgments

This project is funded by ESA MAP A099-075. The authors would like to thank M Scheffer (formerly TU Chemnitz, Germany) for allowing the measurement of the viscosities.

References

[1] Fuganti A 2000 Al foam for automtive applications *Adv. Eng. Mater.* **2** 200–4
[2] Ashby M F *et al* 1998 *Cellular Metals, A Design Guide* (Cambridge: Cambridge University Press)
[3] Stanzick H *et al* 2002 Process control in aluminium foam production using real-time x-ray radioscopy *Adv. Eng. Mater.* **4** 814–23
[4] Stanzick H and Banhart J 2002 Material flow in metal foam studied by neutron radioscopy *Appl. Phys.* A **74** 1118–20
[5] Weaire D and Hutzler S 1999 *The Physics of Foams* (Oxford: Clarendon)
[6] Verbist G, Weaire D and Kraynik A M 1996 The foam drainage equation *J. Phys.: Condens. Matter* **8** 3715–31
[7] Cox S J, Bradley G and Weaire D 2001 Metallic foam processing from the liquid state *Eur. Phys. J. Appl. Phys.* **14** 87–96
[8] Koehler S A, Hilgenfeldt S and Stone H A 2000 A generalized view of foam drainage: experiment and theory *Langmuir* **16** 6327–41
[9] Cox S J *et al* 2000 Applications and generalisations of the foam drainage equation *Proc. R. Soc.* A 2441–64
[10] Gergely V and Clyne T W 2004 Drainage in standing liquid metal foams: modelling and experimental observations *Acta Mater.* **52** 453–63
[11] Brunke O, Odenbach S and Beckmann F 2005 Quantitative methods for the analysis of synchrotron-muCT datasets of metallic foams *Eur. Phys. J. Appl. Phys.* **29** 73–81 (DOI: 10.1051/epjap:2004203)
[12] Brunke O, Odenbach S and Beckmann F 2004 Structural characterization of aluminium foams by means of micro computed tomography *SPIE: Developments in X-Ray Tomography IV* (Denver: SPIE Press) pp 5535453–63
[13] Iida T and Guthrie R I L 1988 *The Physical Properties of Liquid Metals* (Oxford: Clarendon)
[14] Anson J P 1999 The surface tension of molten aluminium and Al–Si–Mg alloy under vacuum and hydrogen atmospheres *Metall. Mater. Trans.* B **30** 999–1027
[15] Babcsán N *et al* 2004 The role of oxidation in blowing of particle stabilised aluminium foams *Adv. Eng. Mater.* **6** 422–7
[16] Koehler S A, Hilgenfeldt S and Stone H A 2004 Foam drainage on the microscale: I. Modeling flow through single Plateau borders *J. Colloid Interface Sci.* **276** 420–38
[17] Carrier V, Destouesse S and Colin A 2002 Foam drainage: a film contribution? *Phys. Rev.* E **65** 061404
[18] Neethling S J 2002 A foam drainage equation generalised for all liquid contents *J. Phys.: Condens. Matter* **14** 331–42